Available online at www.sciencedirect.com
SCIENCE DIRECT®
Journal of Solid State Chemistry 177 (2004) 3310–3315
JOURNAL OF SOLID STATE CHEMISTRY
http://elsevier.com/locate/jssc

Praseodymium magnetic contribution in the low temperature structure of $Pr_{0.8}Ca_{0.2}MnO_3$

Nicolas Guiblin, Dominique Grebille,* Christine Martin, and Maryvonne Hervieu

Laboratoire de cristallographie et Sciences des materiaux (UMR CNRS 6508), Ecole Nationale Superieure d'Ingenieurs de Caen, 6 boulevard du Maréchal Juin, 14050 Caen Cedex, France

Received 16 March 2004; received in revised form 17 May 2004; accepted 23 May 2004

Available online 20 July 2004

Abstract

Magnetic and crystal structures of the manganite $Pr_{0.8}Ca_{0.2}MnO_3$ have been studied by neutron powder and single-crystal X-ray diffraction. Structure refinements using single crystal data [orthorhombic system, *Pnma*, (No. 62), $a_{RT} = 5.5534(3)$ Å, $b_{RT} = 7.6548(8)$ Å, $c_{RT} = 5.4400(5)$ Å, $D_x = 6.422\,g\,cm^{-3}$, $R^{RT} = 0.029$, $R_w^{RT} = 0.038$] are consistent with a single domain sample. Structure and atomic displacement parameters exclude any electronic localization, even in a disordered way at 300 and 100 K. Low temperature electron diffraction observations do not show any trace of charge ordering.

A Pr contribution to the magnetic structure has been shown with a maximum moment of $0.79\,\mu_B$ and spins alignments roughly along [101] orientations, at a lower temperature than the ferromagnetic transition observed at 130 K, due to Mn spins ordering.
© 2004 Elsevier Inc. All rights reserved.

PACS: 75.25.+z; 75.30.Kz; 75.47.Lx

Keywords: Manganites; Magnetoresistance; Magnetic structure; Crystal structure; Magnetism

1. Introduction

Scientific community has dedicated a great interest in the study of manganites perovskites for long years [1]. This is in particular due, more recently, to colossal magnetoresistance (CMR) properties [2–4] found in the case of some compositions $Ln_{1-x}Ae_xMnO_3$ with $Ln = La, Pr, Nd\ldots$ and $Ae = Ca, Sr\ldots$. The work presented here is a part of a more important study on manganites of composition $Pr_{1-x}Ca_x[Mn^{3+}_{1-x}Mn^{4+}_x]O_3$. This Pr–Ca–Mn–O system was chosen because of the absence of size-mismatch between the Pr and Ca cations (respectively, 1.179 and 1.180 Å in ninefold coordination, according to Shannon [5]). This property implies a minimal steric distortion due to the chemical disorder induced on the B-site of the perovskite structure, as a function of the substitution level x. So, the specific physical properties of the related compounds can be attributed to the mixed valence of Mn.

We particularly focused our studies on the $x = 0.2$, 0.3 and 0.4 nominal compositions. As a matter of fact, as shown in the phase diagram of this system [6], the corresponding phases present in this composition range a very large variation in their physical properties, and in particular concerning magnetoresistance phenomena, in connection with a large panel of different nuclear, orbital and spin ordered states. The challenge is to correlate these different points. Those compositions are indeed at the border between two different magnetic behaviors; the first one ($x = 0.2$) is ferromagnetic (FM), the second one ($x = 0.4$) antiferromagnetic (AFM). The intermediate composition ($Pr_{0.67}Ca_{0.33}MnO_3$) shows the coexistence of both ferromagnetism and antiferromagnetism in a complex so-called "red cabbage" system [7]. This phase separation and the associated possible percolation phenomena are invoked to explain colossal magnetoresistance properties.

From the structural point of view, the phase diagram zone $0.3 \leqslant x \leqslant 0.5$ also corresponds to the appearance of a phase transition usually associated to a charge ordering (CO) phenomenon, that is Mn^{3+} ([Ar]$3d^4$)

*Corresponding author. Fax: +33-2-31-95-16-00.
E-mail address: grebille@ismra.fr (D. Grebille).

0022-4596/$ - see front matter © 2004 Elsevier Inc. All rights reserved.
doi:10.1016/j.jssc.2004.05.053

and Mn^{4+}([Ar]$3d^3$) arrangement in the structure, below the CO transition temperature T_{CO}, in those mixed valence compounds. This point is still in discussion and was recently reinterpreted as a partial charge localization via the formation of magnetic bipolarons [8].

For $x \leqslant 0.25$, one observes a ferromagnetic (FM) behavior and the absence of any CO phenomena. This seems to be in contradiction with the insulating character of this compound and with the electric-field-induced nonlinear conduction previously reported [9]. The $Pr_{0.8}Ca_{0.2}MnO_3$ composition shows the higher T_C and magnetization value in the present system [6]. Even if the magnetization value reaches 4 μ_B at 5 T, a metallic state is never obtained. As previously shown [10], only a small kink is observed on the $\rho(T)$ resistivity curve at $\sim$130 K. The FM insulator state is explained by a reduced orbital overlap between Mn and O resulting from important tilt angles in relation with the small average A-site cationic radius, and by the low hole concentration. A recent specific heat study [10] has shown that interactions between the Mn and Pr sublattices have probably to be taken into account to describe the magnetic low temperature contribution.

The structure of the $x = 0.2$ compound was previously refined using neutron powder diffraction data [11]. The evolution of the diffraction data as a function of the temperature is compatible with the existence of two ferromagnetic transitions. The main one can be ascribed to the T_c temperature (140 K) and to the ordering of the Mn spins; the second one (70 K) is very weak and has been attributed to the contribution of the Pr spins.

One specific difficulty for the study of these types of compounds is to combine different structural or physical characterizations with either single crystal or ceramic samples, which are most of the time obtained from different preparations. The aim of the present study was thus to provide both structural and magnetic investigation of the $Pr_{0.8}Ca_{0.2}MnO_3$ phase carried out with samples obtained from the same bulk initial material, a polydomain pseudocubic single crystal rod. A splinter of this rod provided the single crystal studied by X-ray diffraction. Another part was crushed in order to perform measurements by neutron powder diffraction and by electron diffraction. Other physical characterizations were also performed with this same single crystal [12].

2. Sample preparation and characterization

The feeding rod used for the crystal growth has the composition $Pr_{0.8}Ca_{0.2}MnO_3$. A mixture of CaO, prepared by decarbonation of $CaCO_3$ at 1273 K, Pr_6O_{11} and MnO_2 (Aldrich) in stoichiometric proportions was heated to 1273 K and crushed, three times in succession, so as to obtain a good sample homogeneity. It was then compressed in an isostatic press at 3×10^7 Pa in the form of rods (100 mm × ∅ 5 mm) before sintering at 1673 K for 12 h in air.

Crystal growth was carried out in a four-mirror optical floating zone furnace (Crystal Systems, Inc.). The samples were set to rotate in opposite directions at 20 revolutions per minute and were grown in air, at atmospheric pressure, at a feeding speed of 3 mm h^{-1}. So, several-cm-long single crystals were obtained and different samples were collected from the same preparation: small single crystals for X-ray diffraction measurements and crushed samples for neutron diffraction powder measurements.

Magnetization and resistivity curves were recorded using a squid magnetometer and a PPMS system, respectively. Magnetization measurements performed on the present samples clearly show a transition associated to ferromagnetism at $T_c = 130$ K (Fig. 1). This transition is also associated with a small anomaly of the resistivity curve, which disappears under application of a magnetic field of 9 T. Magnetization measurements as a function of the applied field (Fig. 2) show a saturation value of 4.4 μ_B/f.u. This value is larger than the expected one for Mn only, which is equal to 3.8 μ_B/f.u. A more detailed study of the physical properties was previously reported in [12], performed by using a piece of this crystal.

The cationic composition was checked by Energy Dispersive Spectroscopy (EDS) analyses, working with both scanning and transmission electron microscopes. The measurements were carried out on more than 20 particles picked up from different zones of the rod. They confirmed the $Pr_{0.8}Ca_{0.2}Mn$ ratio (calculated for one Mn per formula) and the homogeneous cation distribution of the material, in the limit of accuracy of the technique.

The sample for transmission electron microscopy was prepared by crushing the crystal in alcohol and the small flakes were deposited on a holey carbon film supported

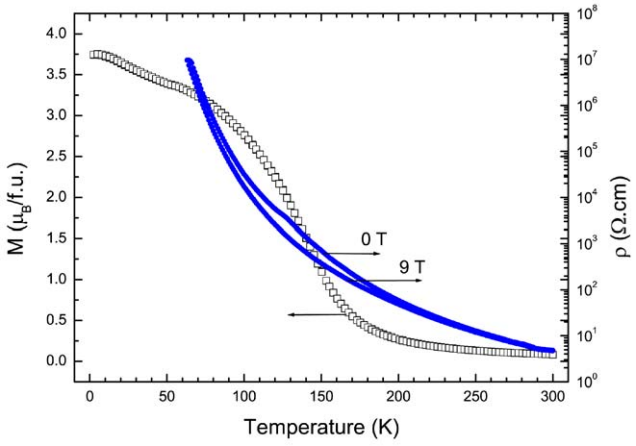

Fig. 1. Magnetization (zfc, 1.45 T) [left y-axis] and resistivity (without magnetic field and in 9 T magnetic field) [right y-axis] vs. temperature.

by a copper grid. The electron diffraction investigation was performed using a JEOL 2010 electron microscope at room temperature and at 10 K, working with a He_{liq} cooling sample holder.

The reconstruction of the reciprocal space was carried out by tilting around the crystallographic axes. It confirmed the orthorhombic cell parameters $(a_p\sqrt{2}, 2a_p, a_p\sqrt{2})$ and the conditions limiting the reflections are consistent with the *Pnma* space group.

Lowering the temperature down to 10 K showed that there is no significant structural modification, retaining the cell symmetry. This is exemplified in the [001] ED pattern given in Fig. 3. One can note the absence of satellites, which are the signature of the charge ordering, or diffuse streaks and the point-like shape of the spots. These observations allow, in agreement with the low temperature lattice images, asserting the absence of short range ordering since the technique is very sensitive to such phenomena.

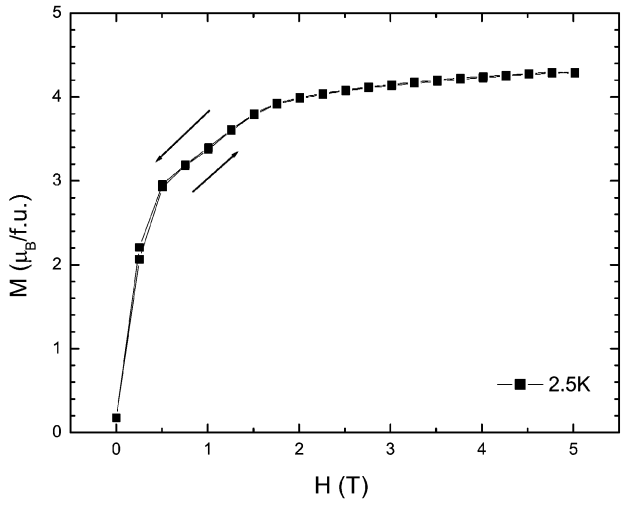

Fig. 2. Magnetization vs. H at 2.5 K.

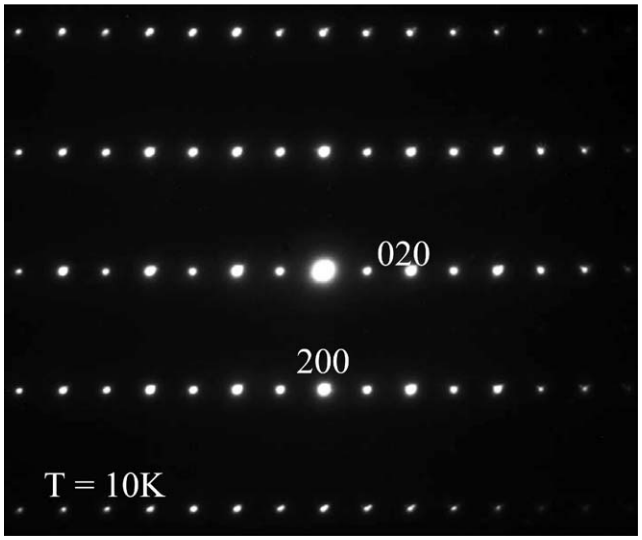

Fig. 3. [001] ED pattern of $Pr_{0.8}Ca_{0.2}MnO_3$ recorded at 10 K: no extra reflections are observed and the conditions of reflection of the *Pnma* space group (*hk*0: $h = 2n$) are retained.

Single crystal data were collected from a small splinter isolated from the original optical furnace rod, at room temperature and at 100 K. A standard structure refinement was performed both at room temperature and at 100 K, with the JANA2000 software [13] ($R = 0.029$ and $R_w = 0.0379$ for the RT data set, and $R = 0.0436$ and $R_w = 0.062$ for the 100 K). The results (deposited at the Inorganic Crystal Structure Database nos CSD numbers 413980 and 413981[1]), for the first time obtained with single crystal data, are quite compatible with previously published results [11] in the orthorhombic *Pnma* symmetry. More important is the observation of the diffraction pattern which is characterized by the absence of reflections (*hk*0) with $h = 2n + 1$ and $k = 2n$, the latters being systematically observed in the case of twinned distorted perovskites. Taking into account the probability of 6 possible symmetry related equivalent orthorhombic domains in relation with the parent cubic structure [14], the refinement, in agreement with the previous observation, definitely proved the monodomain character of this sample. It allows a very accurate and reliable structural description, in particular concerning atomic displacement parameters (Table 1).

Thermal U_{iso} values show a normal decrease with the decrease of the temperature. Anisotropic thermal parameters could also be refined and do not show any significant anomaly. The structure remains very regular. A constant elongation of the MnO_6 octahedra in one of the direction of the equatorial plane can be interpreted as the signature of the Jahn–Teller effect of Mn^{3+}. Only one Mn site is necessary to refine the structure, so that it is not possible to differentiate specific sites for Mn^{3+} or Mn^{4+} species. A possible disorder between two types of octahedra according to a specific local valence of the Mn atom should result in either a split atom model or at least rather big atomic displacement parameters for the O atoms. The corresponding refined values are not in favor of such a description. Considering a unique Mn environment, a bond valence sum can be calculated [15,16] and is found to be 3.29, i.e., very close to the expected value of 3.20. No significant change with temperature could be noticed as far as distances and angles are concerned.

3. Neutron diffraction data, crystal and magnetic structure

Magnetic structure refinement was performed using neutron diffraction data collected at the "Orphée" reactor at the Laboratoire Léon Brillouin (CEA Saclay, France) on the 2-axis diffractometer G4 1 ($\lambda = 2.4266$ Å) in a

[1] ICSD database, FIZ Karlruhe, P.O. Box 2465 D-76012 Karlsruhe.

Table 1
Anisotropic atomic displacement parameters (10^3 Å^2)

Room temperature							
Atom	U_{11}	U_{22}	U_{33}	U_{12}	U_{13}	U_{23}	U_{eq}
Pr/Ca	9.7(1)	6.8(1)	8.7(1)	0	−1.4(1)	0	0.0084
Mn	7.5(2)	4.9(2)	6.3(2)	0.4(1)	0[¤]	0[¤]	0.0063
O_{ap}	11.7(14)	10.8(15)	11.9(13)	0	0[¤]	0	0.012
O^{eq}	11.7(9)	11.9(10)	12.3(9)	−0.14(8)	0.10(8)	0.9(8)	0.012
100 K							
Pr/Ca	6.2(1)	4.8(1)	6.3(1)	0	−0.7(2)	0	0.0059
Mn	5.1(3)	3.6(3)	5.7(3)	0.3(3)	0[¤]	0[¤]	0.0048
O_{ap}	7(2)	13(3)	8(2)	0	0[¤]	0	0.0093
O_{eq}	10(1)	7(1)	9(1)	−1(1)	0[¤]	0[¤]	0.0091

[¤]: Non significant value.

temperature range from 1.5 K to room temperature (RT), by 3 K steps. Data were collected from 2° to 82° in 2θ.

High-resolution-diffraction measurements were also performed with the 2-axis 3T 2 diffractometer ($\lambda = 1.2251$ Å) for crystal and magnetic structure, at RT and 10 K, 2θ range from 6° to 120°. The FullProf [17] program was used to solve both crystal and magnetic structures.

All G4 1 medium resolution data were refined in the orthorhombic *Pnma* symmetry. The evolution (not shown) of the cell parameters from RT to 1.5 K with very small variations and a slope breaking around 135 K, is quite analogous to the previous ones [11]. The ferromagnetic transition does not influence drastically the local environment of the Mn atom but results in a slight and complex change in the slopes of the dilatation curves.

The magnetic transition is also clearly visible by the important contributions of magnetic peaks to nuclear reflections (Fig. 4).

A first approach to the magnetic structure was to introduce a Mn spin ordering only. The different magnetic groups associated with the propagation vector ($k = 0,0,0$) for the ferromagnetic transition and compatible with the *Pnma* space group have been tabulated by Bertaut [18] and lead for the transition element to 4 irreducible representations allowing a non-zero magnetic contribution.

Assuming four 3d cations on equivalent positions labelled as follows:

$$S1: 0\ 0\ \tfrac{1}{2};\quad S2: 0\ \tfrac{1}{2}\ \tfrac{1}{2};\quad S3: \tfrac{1}{2}\ \tfrac{1}{2}\ 0;\quad S4: \tfrac{1}{2}\ 0\ 0.$$

Four base vectors representing the possible magnetic modes of coupling can be expressed according to Bertaut's notation.

$$F = S1 + S2 + S3 + S4,$$

$$G = S1 - S2 + S3 - S4,$$

$$C = S1 + S2 - S3 - S4,$$

$$A = S1 - S2 - S3 + S4.$$

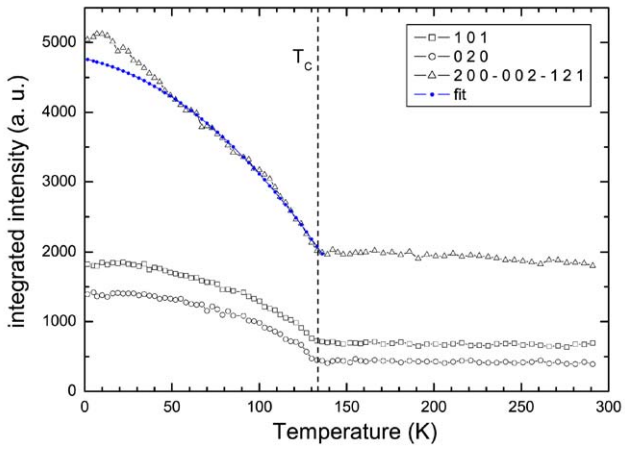

Fig. 4. Integrated intensity vs. temperature, of the (1 0 1), (0 2 0) and (1 2 1)(0 0 2)(2 0 0) peaks (with a fit of this last peak with only a Mn contribution).

Then the different possible coupling modes associated with the *Pnma* symmetry can be derived and are given in Table 2.

The main magnetic intensity contributions are found for the (1 0 1), (0 2 0), (1 2 1 −0 0 2), (2 2 0) and (0 2 2) lines. A structure factor calculation shows that they can only be derived assuming a F coupling mode which is also in agreement with the ferromagnetic character of the compound. No significant magnetic contribution is found for the (2 0 0) line, suggesting a magnetic moment along x. Then, assuming the corresponding Γ_2 representation and refining the x component of the magnetic moment lead to a value of 3.30(4) μ_B at 10 K for a magnetic R_{mag} factor of 0.17.

This poor agreement for lower temperatures can be explained first by a bad adequation of the (1 0 1), (0 2 0) and (2 0 0 −0 0 2−1 2 1) lines as previously mentioned [11], and second by the absence of contribution for small magnetic lines (1 0 0) and (0 2 1) appearing significantly for $T < 50$ K. Refining a z component for the Mn magnetic moment in agreement with a C coupling mode

Table 2
Possible magnetic coupling modes compatible with the 8 irreducible representations of *Pnma*

Representation	Mn			Pr		
	x	*y*	*z*	*x*	*y*	*z*
Γ_1	G	C	A	·	C	·
Γ_2	F	A	C	F	·	C
Γ_3	A	F	G	·	F	·
Γ_4	C	G	F	C	·	F
Γ_5	·	·	·	A	·	G
Γ_6	·	·	·	·	G	·
Γ_7	·	·	·	G	·	A
Γ_8	·	·	·	·	A	·

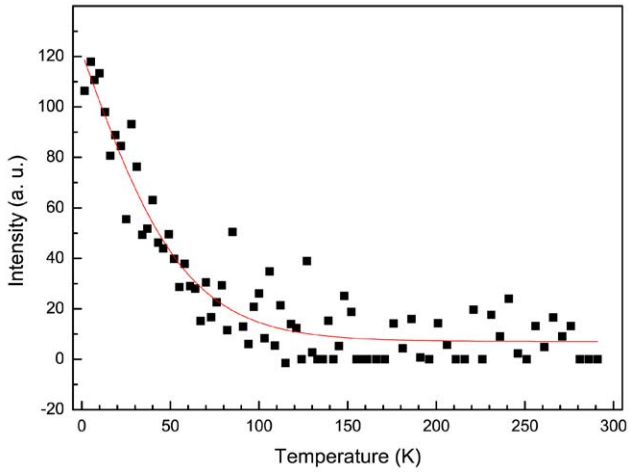

Fig. 5. Evolution of the intensity of the (1 0 0) reflection with the temperature.

(Γ_2 representation) can explain the (1 0 0) and (0 2 1) lines but does not improve significantly the agreement. An A_y magnetic component was also tested and no significant contribution could be found.

As it was proposed by Jirák et al. [19], and already partly tested by Dho et al. [11], a Pr magnetic contribution was assumed, because of a clear evidence of new contribution to the (1 0 0) reflection, as shown in Fig. 5. If we admit exchange interactions between the two magnetic sublattices, this involves a (F_x–C_z) coupling mode compatible with the same Γ_2 representation, without any contribution along *y*, with equivalent positions as follows ($\delta_x = 0.05499$, $\delta_z = 0.01183$, from the 10 K refinement results):

$$S1: 0+\delta_x\ \tfrac{1}{4}\ 0-\delta_z; \quad S2: 0-\delta_x\ \tfrac{3}{4}\ 0+\delta_z;$$
$$S3: \tfrac{1}{2}-\delta_x\ \tfrac{3}{4}\ \tfrac{1}{2}-\delta_z; \quad S4: \tfrac{1}{2}+\delta_x\ \tfrac{1}{4}\ \tfrac{1}{2}+\delta_z.$$

A good agreement ($R_{mag} = 0.021$) was obtained with the refined magnetic components given in Table 3. A *x* ferromagnetic contribution of the Pr atom, and antiferromagnetic *z* contribution of the Pr and Mn atoms have been simultaneously introduced beside the main ferromagnetic *x* Mn contribution. The first one gives a better calculation of the (1 0 1), (0 2 0) and (2 0 0 −0 0 2 −1 2 1) and was the only contribution taken into account by Dho et al. [11]; the second one explains the weak magnetic component (1 0 0) and (0 2 1); the third one gives a better description of the (1 2 0) and (0 2 1) peaks. This is illustrated in Fig. 6 (models 1, 2 and 3, respectively).

The resulting magnetic moment of the Pr atom is 0.79(6) μ_B oriented at 36° from the *a* direction. The corresponding magnetic model is schematically drawn in Fig. 7.

In conclusion, the nuclear and magnetic structures of $Pr_{0.8}Ca_{0.2}MnO_3$ have been revisited. A new magnetic transition is shown at low temperature, involving an ordering of the Pr moments. A symmetry analysis shows that the basis vectors of the Mn and Pr sites belong to the same Γ_2 representation of the *Pnma* group, which was also driving the main T_C ferromagnetic transition, corresponding to the unique Mn ferromagnetic order. This transition clearly involves a coupling between localized 4f spins of Pr atoms and 3d spins of Mn atoms, following now a canted ferromagnetic ordering. No evidence of any charge ordering could be observed, either by electron or X-ray diffraction, as it was proposed for this insulating material [20,21]. Owing to

Table 3
Magnetic components for the different atoms used in the magnetic cell description, obtained at 10 K

	Mn atoms	Pr atoms
M_x	3.38(3)	0.65(3)
M_z	0.17(9)	0.46(11)
M	3.39(3)	0.79(6)

The last row values correspond to the global magnetic moments. Moments are expressed in μ_B.

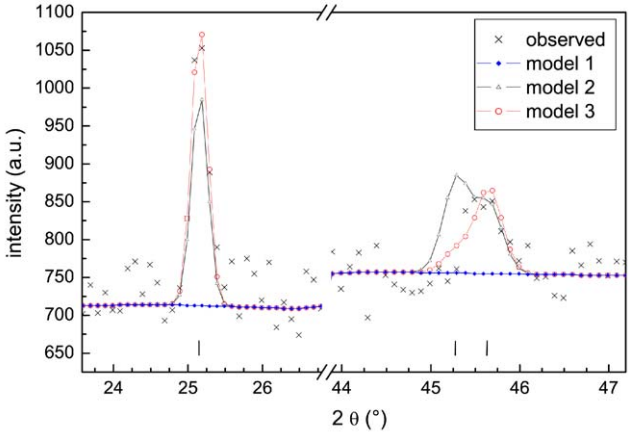

Fig. 6. Representation of (1 0 0), (1 2 0) and (0 2 1) reflections (resp. $2\theta = 25.15°$, 45.29° and 45.65°) for different magnetic contributions along *x*- and *z*-axis, as explained in text.

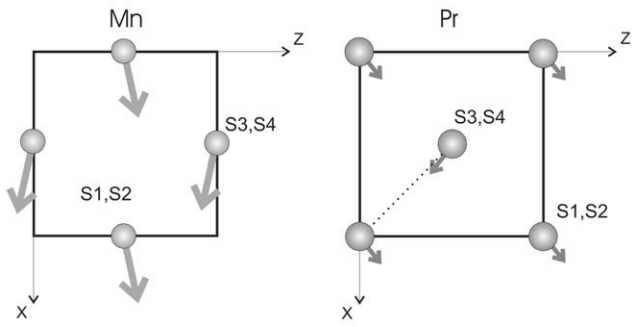

Fig. 7. Schematic projection of the magnetic Mn and Pr structure along the b direction. S1 and S3 Mn (resp. Pr) sites are located at $y=0$ (resp. $\frac{1}{4}$); S2 and S4 Mn (resp. Pr) sites are located at $y=\frac{1}{2}$ (resp. $\frac{3}{4}$).

the structure refinement, the Mn valence cannot be considered as a random distribution of Mn^{3+} and Mn^{4+} but as a real mixed valence 3.2.

Acknowledgments

The authors gratefully acknowledge the Conseil Régional de Basse-Normandie for financial support. They are indebted to Ms. Laurence Hervé and Ms. Josiane Chardon (CRISMAT) for the sample preparation and data collection, respectively, and to Cédric Yaicle and Maud Giot (CRISMAT) for magnetic measurements. They also express their thanks to Gilles André and Françoise Bourée (Laboratoire Léon Brillouin) for neutron diffraction data collections. One author (N.G.) thanks Přemysl Beran (Institute of chemical-technology in Prague, Technická 5, Prague 6, 166 28, Czech Republic) for the help in developing a software for the integrated intensity recovering in all G4 1 diagrams.

References

[1] C.W. Searle, S.T. Wang, Canad. J. Phys. 48 (1969) 2023–2031.
[2] M. Mc Cormack, S. Jin, T.H. Tiefel, R.M. Fleming, J.M. Phillips, Appl. Phys. Lett. 64 (1994) 3045–3047.
[3] R. Mahesh, R. Mahendiran, A.K. Raychaudhuri, C.N.R. Rao, J. Solid State Chem. 114 (1995) 297–299.
[4] B. Raveau, A. Maignan, V. Caignaert, J. Solid State Chem. 117 (1995) 424–426.
[5] R.D. Shannon, C.T. Prewitt, Acta Crystallogr. B 25 (1969) 925–946;
R.D. Shannon, C.T. Prewitt, Acta Crystallogr. B 26 (1970) 1046–1048;
R.D. Shannon, Acta Crystallogr. 32 (1976) 751–767.
[6] C. Martin, A. Maignan, M. Hervieu, B. Raveau, Phys. Rev. B 60 (17) (1999) 12191–12199.
[7] Ch. Simon, S. Mercone, N. Guiblin, C. Martin, A. Brûlet, G. André, Phys. Rev. Lett. 89 (2002) 207202.
[8] A. Daoud-Aladine, J. Rodríguez-Carvajal, L. Pinsard-Gaudart, M.T. Fernandez-Díaz, A. Revcolevschi, Phys. Rev. Lett. 89 (2002) 097205, 129902.
[9] S. Mercone, A. Wahl, Ch. Simon, C. Martin, Phys. Rev. B 65 (2002) 214428.
[10] A. Wahl, V. Hardy, C. Martin, Ch. Simon, Eur. Phys. J. B 26 (2002) 135–140.
[11] J. Dho, E.O. Chi, N.H. Hur, K.W. Lee, H.S. Oh, Y.N. Choi, Solid State Commun. 123 (2002) 441–444.
[12] V. Markovitch, I. Fita, A.I. Shames, R. Puzniak, E. Rozenberg, C. Martin, A. Wisniewski, Y. Yuzhelevskii, A. Wahl, G. Gorodetsky, Phys. Rev. B 68 (2003) 094428.
[13] V. Petříček, M. Dušek, The crystallographic computing system JANA2000. Institute of Physics, Praha, Czech Republic, 2000.
[14] R. Wang, J. Gui, Y. Yhu, A.R. Moodenbaugh, Phys. Rev. B 63 (2001) 144106.
[15] I.D. Brown, D. Altermatt, Acta Crystallogr. B 41 (1985) 244–247.
[16] N.E. Brese, M. O'Keefe, Acta Crystallogr. B 47 (1991) 192–197.
[17] J. Rodríguez-Carvajal, Physica B 192 (1993) 55.
[18] E.F. Bertaut, Acta Crystallogr. A 24 (1968) 217–231.
[19] Z. Jirák, S. Krupička, Z. Šimša, M. Dlouhá, S. Vratislav, J. Magn. Magn. Mater. 53 (1985) 153–166.
[20] D.I. Khomskii, K.I. Kugel, Phys. Rev. B 67 (6) (2003) 134401.
[21] T. Mizokawa, D.I. Khomskii, G.A. Sawatzky, Phys. Rev. B 63 (2000) 024403.